ELSEVIER

Journal of Crystal Growth 236 (2002) 155–164

JOURNAL OF CRYSTAL GROWTH

www.elsevier.com/locate/jcrysgro

Surface morphology of homoepitaxial GaSb films grown on flat and vicinal substrates

B.Z. Nosho[a,*,1], B.R. Bennett[a], E.H. Aifer[a], M. Goldenberg[b]

[a] *Naval Research Laboratory, Code 6876, 4555 Overlook Avenue SW Washington, DC 20375, USA*
[b] *SFA, Inc., Largo, MD 20774, USA*

Received 2 August 2001; accepted 28 November 2001
Communicated by A.Y. Cho

Abstract

We have compared the surface morphology of GaSb homoepitaxial films grown on both flat and 1° vicinal [miscut towards (1 1 1)A] (0 0 1) substrates using atomic force microscopy and scanning tunneling microscopy. Mound formation is observed for GaSb homoepitaxy on the flat substrates over a range of growth temperatures when either Sb_2 or Sb_4 is used to supply the group V flux. At sufficiently high growth temperatures, which are different depending on whether Sb_2 or Sb_4 is used, the mounds transform into fairly well-defined pyramids comprised of distinctly stacked layers that are clearly separated by monolayer-height steps. Furthermore, at the tops of the pyramids are sharp, tower-like features that are ~15 Å in height. Mounds also appear during homoepitaxy on the vicinal substrates at lower growth temperatures; however, both mounds and pyramids can be suppressed when using either Sb_2 or Sb_4 by growing at temperatures above ~400°C. We discuss and compare qualitatively the shape of the observed mounds with predictions of evolving morphology based on models of unstable epitaxial growth.

PACS: 61.16.C; 81.15.H; 68.35.B

Keywords: A1. Atomic force microscopy; A1. Surface structure; A3. Molecular beam epitaxy; B1. Antimonides

1. Introduction

The "6.1 Å" family of compound semiconductors, namely InAs, GaSb, and AlSb, and their related alloys, offer much flexibility in heterostructure design due to the near lattice match and variety of band alignments that are possible. A key issue when designing and creating these heterostructures, particularly in samples containing many repeating periods, is balancing the overall strain to minimize dislocation formation. It is thus desirable to grow on substrates close to the 6.1 Å lattice constant to promote coherently strained heteroepitaxy. (In cases requiring semi-insulating substrates, 6.1 Å materials are generally grown on mismatched GaAs or InP substrates.) Presently,

*Corresponding author. Tel.: +1-310-317-5295; fax: +1-310-317-5450.
E-mail address: bzNosho@HRL.com (B.Z. Nosho).
[1] Present address. HRL Laboratories, LLC, Malibu, CA 90265.

0022-0248/02/$ - see front matter
PII: S0022-0248(01)02392-2

Report Documentation Page

Form Approved
OMB No. 0704-0188

1. REPORT DATE	2. REPORT TYPE	3. DATES COVERED
AUG 2001		**00-00-2001 to 00-00-2001**

4. TITLE AND SUBTITLE	5a. CONTRACT NUMBER
Surface morphology of homoepitaxial GaSb films grown on flat and vicinal substrates	5b. GRANT NUMBER
	5c. PROGRAM ELEMENT NUMBER
6. AUTHOR(S)	5d. PROJECT NUMBER
	5e. TASK NUMBER
	5f. WORK UNIT NUMBER
7. PERFORMING ORGANIZATION NAME(S) AND ADDRESS(ES) **Naval Research Laboratory,Code 6876,4555 Overlook Avenue SW,Washington,DC,20375**	8. PERFORMING ORGANIZATION REPORT NUMBER
9. SPONSORING/MONITORING AGENCY NAME(S) AND ADDRESS(ES)	10. SPONSOR/MONITOR'S ACRONYM(S)
	11. SPONSOR/MONITOR'S REPORT NUMBER(S)

12. DISTRIBUTION/AVAILABILITY STATEMENT
Approved for public release; distribution unlimited

13. SUPPLEMENTARY NOTES

14. ABSTRACT
see report

15. SUBJECT TERMS

16. SECURITY CLASSIFICATION OF:			17. LIMITATION OF ABSTRACT	18. NUMBER OF PAGES	19a. NAME OF RESPONSIBLE PERSON
a. REPORT	b. ABSTRACT	c. THIS PAGE			
unclassified	**unclassified**	**unclassified**	**Same as Report (SAR)**	**10**	

the two commercially available substrates near the 6.1 Å lattice constant are InAs and GaSb. Since the lattice constant of GaSb is between that of InAs and AlSb, it is often more desirable to grow on GaSb substrates for lattice matching and strain compensation.

In previous years, growth on many commercially available GaSb substrates had been plagued by the formation of large oval defect mounds observed during homoepitaxy. The defect mounds can vary greatly in size, but generally grow larger with increasing film thickness. In Figs. 1(a) and (b), we show atomic force microscopy (AFM) images of defect mounds of various sizes. These large defects have been shown to be particularly detrimental to the performance of infrared detectors based on InAs/Ga(In)Sb superlattices [1]. Recently, it has been demonstrated that these defect mounds are attributable to disrupted growth over residue, primarily silica particles, that were left behind from the polishing process [2]. Since then, manufacturers have implemented improvements into the rinsing process to minimize polishing residue.

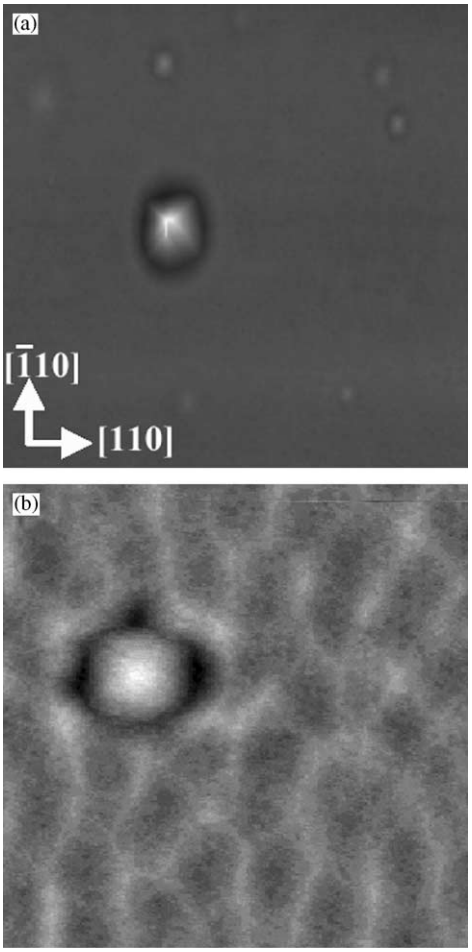

Fig. 1. (a) AFM image (10 μm × 10 μm) of a 0.5 μm GaSb film showing large defect mounds of various sizes. (b) A higher magnification image (5 μm × 5 μm) of one of the smaller mounds shown in (a). The height scales of the images are (a) 20 and (b) 4 nm. The mounds have been shown to nucleate over polishing residue.

With the problem of the large oval defects ostensibly under control, we focus our attention on characterizing the evolving morphology of GaSb homoepitaxial films with the goal of obtaining smooth buffer layers. The growth of semiconductor films by molecular beam epitaxy (MBE) is generally envisioned to form relatively smooth surfaces during homoepitaxy. However, there has been substantial experimental evidence in the literature that unstable growth can arise even during homoepitaxial semiconductor growth [3–5] and lead to the formation of mounds. While these mounds are much smaller than the aforementioned defect mounds, it is clearly desirable to minimize any surface roughness during the fabrication of heterostructures to preserve layers of uniform thickness. In this study, we focus on examining GaSb films over a range of growth conditions as an initial step towards identifying fundamental aspects that influence GaSb epitaxial growth. In particular, we compare the surface morphology of GaSb films grown on flat and vicinal substrates while varying both growth temperature and group V molecular species, i.e., Sb_2 versus Sb_4.

2. Experiment

The samples were grown in a solid-source III–V MBE machine equipped with separate cells to produce Sb_2 and Sb_4 fluxes. [In this paper, we refer to the species produced from the antimony cracker as Sb_2, although calculations [6] and experimental results [7] suggest that both dimers (Sb_2) and monomers (Sb) may be present under our operating conditions.] The "epi-ready" GaSb(0 0 1)

substrates used were either nominally flat or vicinal with a 1° miscut towards (1 1 1)A. This miscut, which creates terraces that are nominally ~172 Å in width in the [1 1 0] direction, was chosen since the anisotropic islands that form during antimonide growth are longer in the [1 1 0] direction [8,9]. A custom-designed holder was used to mount the two different substrates simultaneously and thus allow for a direct comparison of substrate orientation at a given growth condition. Note that when grown separately, we have not observed any differences between the flat and vicinal wafers in terms of oxide desorption and phase transition temperatures. Following thermal oxide desorption at ≈530°C, the GaSb films were grown at various substrate temperatures at a growth rate of 0.5 ML/s with a 2:1 Sb:Ga true flux ratio. The GaSb growth rate was determined from reflection high-energy electron diffraction (RHEED) oscillations and the Sb flux was determined by finding several points at which the growth had become group V limited. Thus, an Sb flux of "1 ML/s" would be just sufficient to sustain a growth rate of 1 ML/s. The samples were quenched (substrate heater power to zero) under a 1 ML/s Sb flux immediately following the growth. The Sb shutter was closed when the substrate temperature reached ≈200°C. Samples studied by scanning tunneling microscopy (STM) were transferred in vacuo to the analysis chamber. All other samples were characterized in air by AFM.

3. Results and discussion

In Fig. 2, we show a series of AFM images that illustrate the different surface morphologies of 0.5 μm GaSb films grown on both flat [Figs. 2(a)–(d)] and vicinal [Figs. 2(e)–(h)] GaSb substrates at various substrate temperatures. To help facilitate comparison of the relative surface roughness, the height scale of all the images except Figs. 2(d) and (e) is 7.5 nm. Due to the larger range in the topography, these two images are displayed using a height range of 15 nm. The differences in the evolving morphology as a function of growth temperature are readily apparent for both types of substrates.

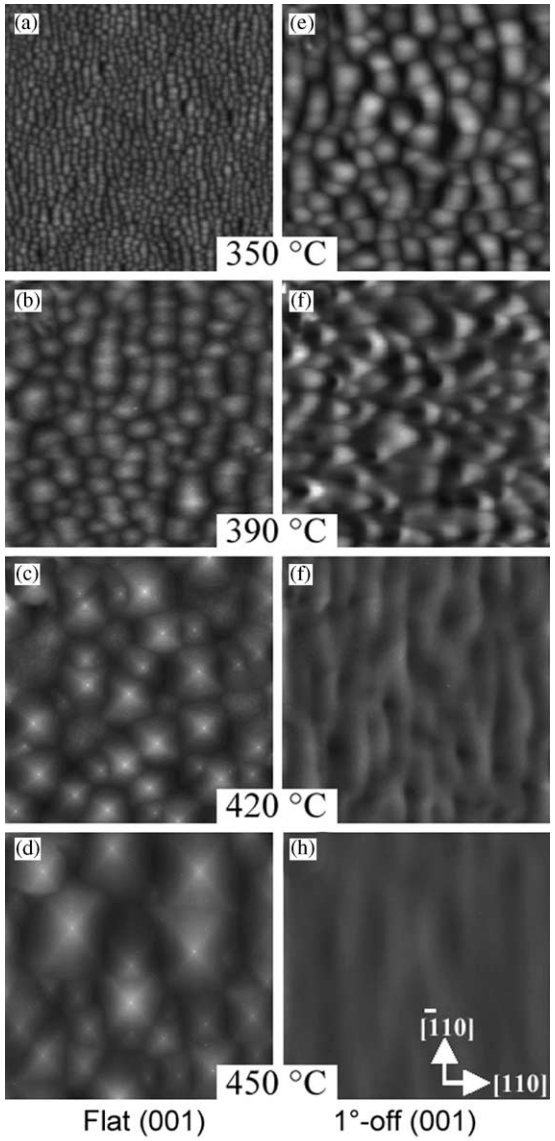

Fig. 2. AFM images (5 μm × 5 μm) of 0.5 μm GaSb films grown using Sb_2 on (a–d) flat and (e–h) 1° vicinal GaSb(0 0 1) substrates; the height scale in (d) and (e) is 15 nm and is 7.5 nm in the others.

On the flat substrates, we always observe the presence of mounds on the surface. As the growth temperature increases, the density of the mounds decreases while both the perimeter and vertical height of the mounds increases. In Figs. 2(a) and (b), the mounds exhibit a hemispherical-type shape that results in a "cobblestone"-like appearance of

the surface. In this case, the hemispherical shape is likely an imaging artifact that is due to the lateral resolution of the AFM probe tip. By a growth temperature of 420°C or higher [Figs. 2(c)–(d)], the shape of the mounds resembles a pyramid-type structure with a square or rectangular base.

There are many reports in the literature describing the formation of mounds. In these reports, two basic mechanisms have been shown to lead to mound formation. The first, and more common explanation, is the presence of the Ehrlich–Schwoebel (ES) barrier at the down step that effectively creates a bias for adatoms moving across, or incorporating into, steps [10,11]. The increased barrier at the down step reduces the attachment to the lower step, thus in turn increasing the attachment into the up-steps. Since adatoms cannot diffuse as easily down steps to equalize the terraces, the tendency is to grow upwards and form the mounds [3,12–15]. The second mechanism for mound formation involves the diffusion of adatoms along step edges [16,17]. When there are asymmetric diffusion processes along steps due to corners or kinks, there is a tendency for adatoms to move closer to the step (and to higher coordinated sites) rather than move away or off the step. The net result is an "uphill" current that can also lead to mound formation. Indeed, it has been demonstrated that mounds can form by this mechanism without the presence of an ES barrier.

A higher magnification view of the pyramid mounds in Figs. 2(c) and (d) are shown in Figs. 3(a) and (d), respectively. To illustrate the morphology more clearly, these figures are also presented as derivative images in Figs. 3(b) and (e) and three-dimensional renderings in Figs. 3(c) and (f), respectively. The pyramids are comprised of concentric layers that form a "wedding cake" structure, where each flat terrace is separated by monolayer-height (~ 3 Å) steps. Although similar in appearance, this type of mound morphology is different from the spiral mounds that form and grow around screw dislocations during GaSb growth on GaAs [18–20] in that each layer is clearly distinct from the others. Furthermore, the widths of the terraces on the pyramids appear remarkably uniform in both the [1 1 0] and [$\bar{1}$ 1 0] directions. While the formation and evolution of mounds reflect kinetic aspects of growth, the pyramids and regularly spaced terraces are more indicative of equilibrium structures.

At the tops of the pyramid mounds, there additionally appear to be sharp, narrow towers, or "flagpole"-like structures, that are ~ 15 Å in height. While flagpoles appear at all the pyramid peaks, we note that this is not the only place where they are observed. This is particularly clear in Figs. 3(d) and (e) where many of the flagpoles are not at pyramid peaks. We believe that these flagpoles likely resulted from the coalescence of pyramids as they grew larger and eventually into each other. In the circled areas in Figs. 3(d) and (e), the tops of pyramids that have not yet been fully incorporated into neighboring pyramids are just observable. It is also interesting that there are still observable flagpoles at many places where there is no other evidence of the pyramid upon which it was presumably created. This raises the question as to what happens to the towers as pyramids meet and coalesce. If the flagpoles all initially nucleate at the tops of pyramid mounds, this could imply that they are not easily grown over and, to some degree, continue to advance with the surface. These towers are clearly undesirable features for buffer layers where flat surfaces are generally preferred. Furthermore, these features may also adversely affect the properties of a heterostructure by, for example, influencing the epitaxy locally or offering other paths for carriers through heterostructures.

The towers that form at the top of the pyramids are reminiscent of structures predicted by kinetic models that implement an ES barrier [3,12–15]. In a "minimal" model of epitaxial growth, Krug investigated the evolving surface morphology when interlayer transport, i.e., transport across steps, was completely inhibited by an infinite ES barrier [12]. The result was the emergence of sharp peaks or towers at the tops of the mounds that strongly resemble the flagpole structures that we observe. However, while the qualitative agreement describing the flagpoles is reasonable, further attempts to fit the shape of the observed pyramid structure to the shape predicted analytically by this simple model did not yield satisfactory agreement

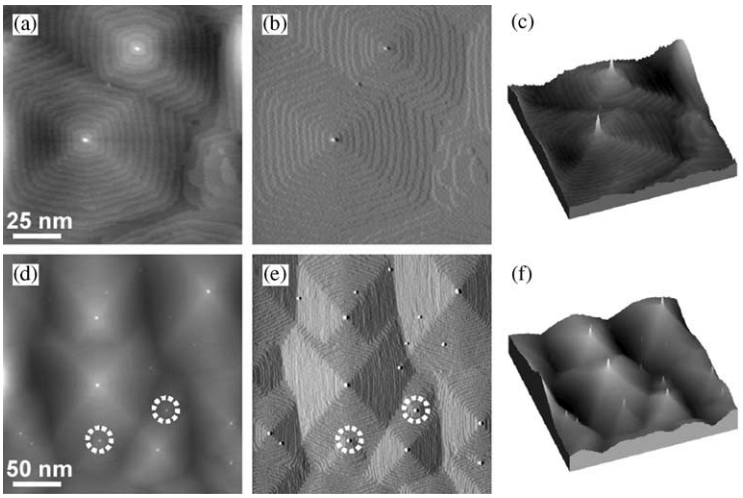

Fig. 3. (a) A high magnification view of a pyramid from Fig. 2(c) showing the concentric layer structure. In (b) and (c) are shown a derivative view and three-dimensional rendering, respectively, of the image in (a). (d) A 2.5 μm × 2.5 μm AFM image of the pyramids in Fig. 2(d), also shown with a derivative and three-dimensional view in (e) and (f), respectively. In (d–f), it is evident that some flagpoles are located at positions other than at the peaks of the pyramids; the circled peaks appear to be remnants from a pyramid that has been grown over by another.

in the surface morphology. The infinite ES barriers preclude the possibility of an incorporation mechanism to lower terraces. As a result, the mounds would tend to grow in height, and would also fill in the lower terraces slowly. This phenomenon, referred to as the ''Zeno effect'', would result in deep cracks forming between the mounds [21]—a morphological feature that is not observed. Other models that include edge diffusion have avoided forming these cracks, indicating that there is some contribution likely from this effect. This would seem reasonable given the lack of evidence pointing towards large ES barriers on semiconductor surfaces.

One possibility for avoiding potential pitfalls that might arise due to mounds or flagpoles is the use of thin buffer layers. In addition, examination of thin films may provide insight towards the early stages of mound formation. It is well known that thermally removing the oxide on semiconductor substrates often creates a substantial amount of surface roughness. Following oxide removal, a buffer layer is usually grown both to smoothen the surface as well as to add distance from the contamination at the substrate–epilayer interface. An AFM image of a GaSb substrate after oxide removal is shown in Fig. 4(a). The roughness appears uniform across the surface and the topography range of the image is 50 nm. Typical line profiles across the surface reveal corrugations on the surface of order 15 nm. After a growth of 300 Å of GaSb [Fig. 4(b)], the surface already appears to have smoothed out much of the roughness from oxide removal, but it is also apparent that the pyramid mounds have already begun to form. There are also several examples of the early stages of pyramid growth that appear as two or three stacked layers. It is clear in Fig. 4(b) that the surface is much flatter than the 0.5 μm GaSb film grown under nominally identical conditions [Fig. 2(d)]. Furthermore, the mounds that have formed on the thin buffer layer are much smaller and do not exhibit any evidence of flagpoles.

Another possibility for preventing or limiting mound formation is to grow on vicinal substrates. Studies of GaAs epitaxy have shown that RHEED oscillations decay more quickly, or are absent, for growth on vicinal substrates under conditions similar to those that would result in oscillations on nominally flat substrates [22]. The interpretation of this result was that the higher step density

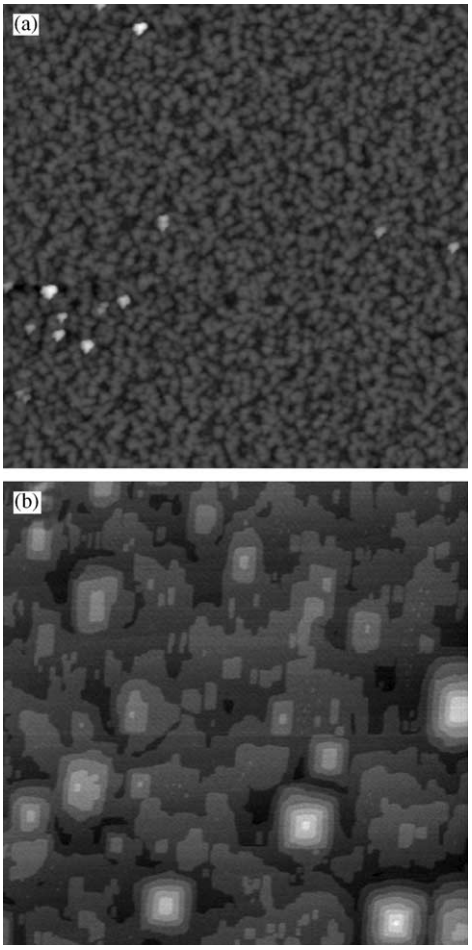

Fig. 4. AFM images (5 μm × 5 μm) of a GaSb substrate after: (a) oxide removal and (b) growth of 300 Å of GaSb. The height scale in (a) is 50 nm.

promotes step-flow growth by decreasing the diffusion length required for adatoms to diffuse and incorporate into steps. Preliminary measurements in our laboratory suggest that GaSb homoepitaxy is similar as RHEED oscillations are more easily observed on nominally flat GaSb(0 0 1) substrates than on vicinal substrates. While this appears to be initially promising, the instability of step-flow growth on vicinal surfaces was first examined in detail by Bales and Zangwill [23]. Although step-flow growth on vicinal surfaces has generally been regarded to be stable [3], the analysis of Bales and Zangwill surmised that with increasing deposition flux, the nature of growth on a vicinal surface progresses from stable step flow to both unstable step flow and even two-dimensional nucleation. The trend we observe in morphology in Figs. 2(e)–(h) shows good agreement with this supposition since both increasing deposition flux and decreasing growth temperature should affect growth similarly by decreasing the ratio of surface diffusion to deposition flux. The observation of mound formation on the vicinal substrates in Figs. 2(e) and (f) indicates that at these lower growth temperatures, the growth of GaSb is more diffusion limited.

At higher growth temperatures [Figs. 2(g) and (h)], the surfaces appear smoother and the mounds are no longer observed. While these surfaces appear to be textured with patches of depressed areas, we note that this is an artifact of image flattening. A higher magnification view of the surface in Fig. 2(g) is shown in Fig. 5(a). The observable steps, which nominally run vertically in this image and are just barely resolvable, indicate that at these conditions, the surface has evolved in a step-flow manner. The depressed areas are local regions that have a higher step density than that of the actual miscut. This is more clearly illustrated in Fig. 5(b) by a plan-view STM image of a GaSb film grown at $\sim$450°C. It is evident that all the surface steps decline in the same direction and that the contrast changes observed are due to the changes in step density. This morphology agrees well with models of unstable step-flow growth where the step meandering can create ripples on the surface [24].

It has long been realized that the group V molecular species, i.e., monomer, dimer, or tetramer, is a growth parameter that can affect epitaxial growth and device properties [25–29]. These studies illustrated that by varying the group V species during homoepitaxial growth, notable differences could be observed both during growth by RHEED oscillations as well as post-growth by characterization of the evolving surface structure or device properties. In heteroepitaxy, the scenario can be even more complicated, particularly in structures containing both As and Sb, as the choice of group V species affects not only the growth of a given layer, but can also influence the

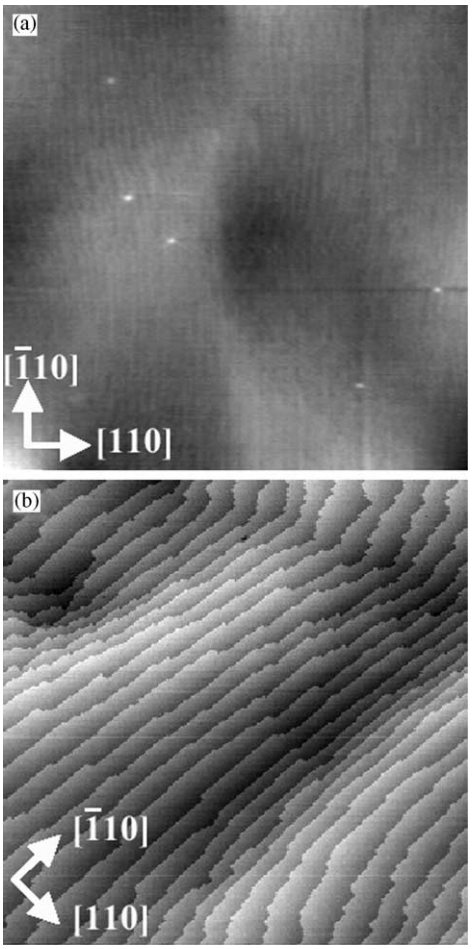

Fig. 5. (a) A higher magnification AFM image (1.2 μm × 1.2 μm) of the surface shown in Fig. 2(g). (b) Plan-view STM image (150 nm × 150 nm) of a thin GaSb film grown at ~450 °C. Some areas appear darker, or depressed, after a plane subtraction due to a higher local step density.

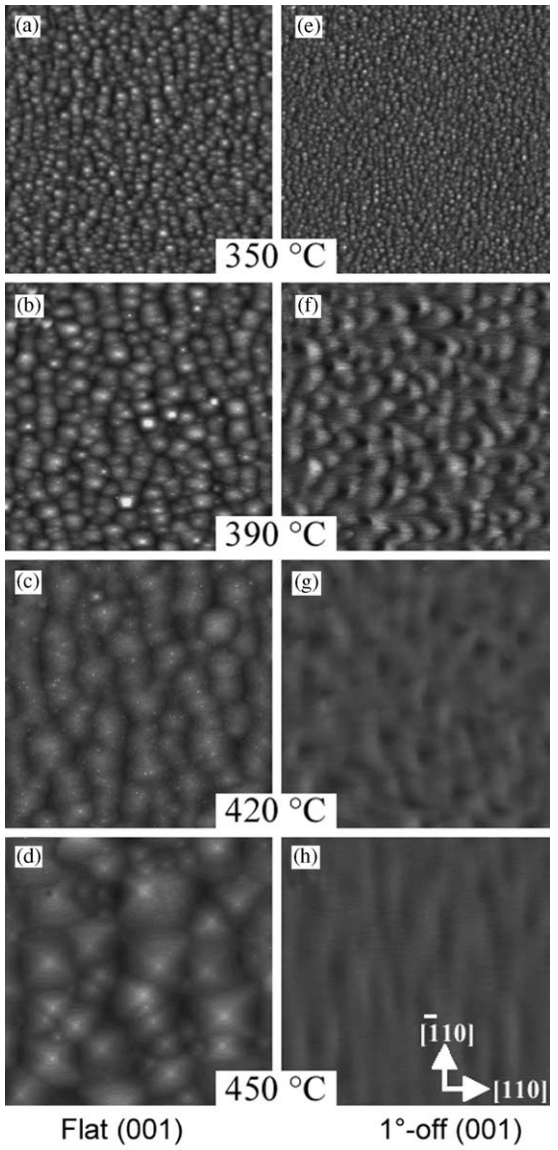

Fig. 6. AFM images (5 μm × 5 μm) of 0.5 μm GaSb films grown using Sb_4 on (a–d) flat and (e–h) 1° vicinal GaSb(0 0 1) substrates. The height scale in (a) and (e) is 15 nm and is 7.5 nm in the others.

degree of anion exchange at interfaces [30–34]. Since tetramers are generally found to be less reactive than dimers in exchange reactions, there are potential advantages to growing with tetramer species. To this end, we examined the surface morphology of GaSb films grown using Sb_4.

In Fig. 6, we show a series of AFM images grown under the same conditions as those in Fig. 2, but using Sb_4 instead of Sb_2. The height scale for all the images is 7.5 nm, except for Figs. 6(a) and (e), which have a height scale of 15 nm due to their larger range in topography. Although we have found that films grown with Sb_4 are slightly smoother in terms of RMS roughness, the use of Sb_2 or Sb_4 during growth does not appear to dramatically affect the qualitative

morphology of GaSb films grown on the vicinal substrates [Figs. 6(e)–(g)]. Interestingly, when comparing growth on flat substrates, we find clearly different trends in the morphology with temperature when Sb_4 [Figs. 6(a)–(c)] rather than Sb_2 [Figs. 2(a)–(c)] is used. While growth with Sb_2 results in the pyramid mounds that increase in size as the growth temperature is increased, growth with Sb_4 yields surfaces that get smoother with increasing temperature over this range. Although the bases of the mounds are generally larger, the heights of the mounds are decreasing, giving rise to the decreasing RMS roughness.

These differing trends on flat substrates seem to indicate that significant differences in the Sb_2 versus Sb_4 incorporation mechanisms may exist and are possibly affecting the diffusion of Ga over or along the steps. As discussed above, these are the two known mechanisms that drive unstable epitaxy and mound formation. It is possible that the surface diffusion, which must play a critical role in pyramid formation, can differ when Sb_4 is used versus Sb_2. When group III atoms attach onto steps, there must also be a sufficient surface flux of group V atoms present to incorporate and fix the atoms into the step. When there are not sufficient group V atoms available, the group III atoms may be able to detach more easily from the step [35]. Since group V tetramers incorporate via a second-order reaction, it is possible that atoms detach from steps (perhaps minimizing mound formation) more easily when using tetramers as compared to equivalent fluxes of dimers. In another study of GaAs epitaxy, Tersoff, Johnson and Orr have indicated that MBE growth can take place close to equilibrium [36]. From this, it follows that the Ga chemical potential, which drives surface diffusion, depends not only on the As pressure, but also on the As molecular species. Although no equivalent comparison of theory and experiment has been yet done for GaSb, an analogous picture would also indicate a dependence of the Ga surface diffusion on the Sb flux and species.

At the highest growth temperature examined [Fig. 6(d)], an interesting change occurs in the morphological trend as the mounds have not only increased in size but have also developed into the pyramid structures that were described earlier when Sb_2 was used during growth. This transition from the "rounded" mounds to the well-defined pyramids was observed at a higher temperature than when Sb_2 was used. If surface diffusion drives the mound formation, then one possible scenario is that Sb_4 has changed the minimal growth temperature required to lead to pyramid formation. Another possibility is that the incorporation kinetics of Sb_4 has substantially changed due to the increased substrate temperature. At growth temperatures above $\sim 450^{\circ}C$, the trend in morphology is similar to that observed when Sb_2 is used (well-defined pyramids increasing in size) indicating that growth with Sb_4 has begun to behave qualitatively similar to growth with Sb_2. This type of qualitative change in the growth behavior with increasing temperature has also been observed recently in film stability studies comparing the effect of As_4 versus As_2 on InAs/GaSb superlattices [34]. Unfortunately, studies detailing the group V incorporation mechanisms on (0 0 1) surfaces have revolved primarily around GaAs growth [26,28,37–39], with little attention having been devoted towards antimonides. Although some kinetic models of the As incorporation kinetics have been fit reasonably well for GaAs for limited scenarios, it is still unclear if analogous mechanisms even exist for antimonide growth. Furthermore, even if the mechanisms are similar, it is still not clear how substrate temperature might affect the adsorption, and possibly cracking, of tetramers on the surface as group V atoms are incorporated during growth.

4. Conclusions

We have used scanning probe microscopy to characterize experimentally the surface morphology of GaSb homoepitaxial films grown on both flat and vicinal (0 0 1) substrates using both Sb_2 and Sb_4. When using Sb_2, we always observe the presence of mounds on the flat substrates. At lower growth temperatures ($\sim 390^{\circ}C$ and lower), the mounds have a more rounded appearance with details of step structure difficult to discern with AFM. At higher growth temperatures, the mounds

evolve as pyramids comprised of distinctly stacked layers that are clearly separated by monolayer-height steps. Furthermore, as the growth temperature is increased, the mound and pyramid sizes increase while the density decreases. Interestingly, at the tops of the pyramids, there are sharp, tower-like features that are ~ 15 Å in height.

When changing the molecular group V species used during growth from Sb_2 to Sb_4, we again observe the presence of mounds on the flat substrates at all temperatures examined. However, in contrast to growth using Sb_2, we find that the height of the mounds (as well as the RMS roughness) decreases as the growth temperature is increased from 350°C to 420°C. A further increase in growth temperature to 450°C changes the morphology as the mounds have changed to the pyramid structure and have begun to increase in size.

The surface morphologies of GaSb homoepitaxial films grown on the vicinal substrates are qualitatively similar when either Sb_2 or Sb_4 is used. Up to ~ 390°C, a high density of mounds is observed that likely indicates a diffusion-limited nature to the growth. At higher temperatures, mound and pyramid formation is suppressed for both Sb_2 and Sb_4 as the growth has proceeded in a step-flow manner resulting in much smoother surfaces with clearly observable steps.

Acknowledgements

The authors thank M.F. Gyure for many fruitful discussions and M.E. Twigg for a critical reading of the manuscript. This work was supported by the Office of Naval Research and an NRC/NRL Postdoctoral Research Associateship (B.Z.N.).

References

[1] E.H. Aifer, B.R. Bennett, B.Z. Nosho, M.E. Twigg, I. Vurgaftman, J.R. Meyer, J.R. Waterman, M. Goldenberg, in: IRIA Center (Ed.), 2001 MSS Specialty Groups on Passive Sensors; Camouflage, Concealment and Deception; Detectors; and Materials, Vienna, VA, filename MTC02EA.pdf, 2001.
[2] A.D. Johnson, unpublished.
[3] M.D. Johnson, C. Orme, A.W. Hunt, D. Graff, J. Sudijono, L.M. Sander, B.G. Orr, Phys. Rev. Lett. 72 (1994) 116.
[4] C. Orme, M.D. Johnson, J.L. Sudijono, K.T. Leung, B.G. Orr, Appl. Phys. Lett. 64 (1994) 860.
[5] J.E.V. Nostrand, S.J. Chey, D.G. Cahill, Phys. Rev. B 57 (1998) 12536.
[6] Y. Rouillard, B. Lambert, Y. Toudic, M. Baudet, M. Gauneau, J. Crystal Growth 156 (1995) 30.
[7] P.D. Brewer, D.H. Chow, R.H. Miles, J. Vac. Sci. Technol. B 14 (1996) 2335.
[8] W. Barvosa-Carter, A.S. Bracker, J.C. Culbertson, B.Z. Nosho, B.V. Shanabrook, L.J. Whitman, Phys. Rev. Lett. 84 (2000) 4649.
[9] A.S. Bracker, B.Z. Nosho, W. Barvosa-Carter, L.J. Whitman, B.R. Bennett, B.V. Shanabrook, J.C. Culbertson, Appl. Phys. Lett. 78 (2001) 2440.
[10] G. Ehrlich, F.G. Hudda, J. Chem. Phys. 44 (1966) 1039.
[11] R.L. Schwoebel, E.J. Shipsey, J. Appl. Phys. 37 (1966) 3682.
[12] J. Krug, J. Stat. Phys. 87 (1997) 505.
[13] M. Biehl, W. Kinzel, S. Schinzer, Europhys. Lett. 41 (1998) 443.
[14] P. Šmilauer, D.D. Vvedensky, Phys. Rev. B 52 (1995) 14263.
[15] S. Schinzer, S. Köhler, G. Reents, Eur. Phys. J. B 15 (2000) 161.
[16] O. Pierre-Louis, M.R. D'Orsogna, T.L. Einstein, Phys. Rev. Lett. 82 (1999) 3661.
[17] M.V. Ramana Murty, B.H. Cooper, Phys. Rev. Lett. 83 (1999) 352.
[18] B. Brar, D. Leonard, J.H. English, Inst. Phys. Conf. Ser. 141 (1995) 335.
[19] B. Brar, D. Leonard, Appl. Phys. Lett. 66 (1995) 463.
[20] P.M. Thibado, B.R. Bennett, M.E. Twigg, B.V. Shanabrook, L.J. Whitman, J. Vac. Sci. Technol. A 14 (1996) 885.
[21] I. Elkinani, J. Villain, J. Phys. I France 4 (1994) 949.
[22] J.H. Neave, P.J. Dobson, B.A. Joyce, J. Zhang, Appl. Phys. Lett. 47 (1985) 100.
[23] G.S. Bales, A. Zangwill, Phys. Rev. B 41 (1990) 5500.
[24] M. Rost, P. Šmilauer, J. Krug, Surf. Sci. 369 (1996) 393.
[25] D.H. Chow, H.L. Dunlap, W. Williamson III, S. Enquist, B.K. Gilbert, S. Subramaniam, P.-M. Lei, G.H. Bernstein, IEEE Electron Device Lett. 17 (1996) 69.
[26] M. Itoh, G.R. Bell, A.R. Avery, T.S. Jones, B.A. Joyce, D.D. Vvedensky, Phys. Rev. Lett. 81 (1998) 633.
[27] E.S. Tok, J.H. Neave, J. Zhang, B.A. Joyce, T.S. Jones, Surf. Sci. 374 (1997) 397.
[28] G.R. Bell, M. Itoh, T.S. Jones, B.A. Joyce, Surf. Sci. 423 (1999) L280.
[29] J.C. Garcia, A.C. Beye, J.P. Contour, G. Neu, J. Massies, A. Barski, Appl. Phys. Lett. 52 (1988) 1596.
[30] M.W. Wang, D.A. Collins, T.C. McGill, R.W. Grant, J. Vac. Sci. Technol. B 11 (1993) 1418.
[31] D.A. Collins, M.W. Wang, R.W. Grant, T.C. McGill, J. Vac. Sci. Technol. B 12 (1994) 1125.

[32] B.R. Bennett, B.V. Shanabrook, M.E. Twigg, J. Appl. Phys. 85 (1999) 2157.
[33] R. Kaspi, J. Crystal Growth 201/202 (1999) 864.
[34] B.Z. Nosho, B.R. Bennett, L.J. Whitman, M. Goldenberg, unpublished.
[35] T. Nishinaga, X.Q. Shen, D. Kishimoto, J. Crystal Growth 163 (1996) 60.
[36] J. Tersoff, M.D. Johnson, B.G. Orr, Phys. Rev. Lett. 78 (1997) 282.
[37] E.S. Tok, T.S. Jones, J.H. Neave, J. Zhang, B.A. Joyce, Appl. Phys. Lett. 71 (1997) 3278.
[38] V.V. Preobrazhenskii, M.A. Putyato, O.P. Pchelyakov, B.R. Semyagin, J. Crystal Growth 201/202 (1999) 170.
[39] J.C. Garcia, C. Neri, J. Massies, J. Crystal Growth 98 (1989) 511.